Available online at www.sciencedirect.com
ScienceDirect
Catalysis Today 120 (2007) 35–44
CATALYSIS TODAY
www.elsevier.com/locate/cattod

Microreactor development for Martian in situ propellant production

J.D. Holladay [a,*], K.P. Brooks [a], R. Wegeng [a], J. Hu [a], J. Sanders [b], S. Baird [b]

[a] *Pacific Northwest National Laboratories, P.O. Box 999, Richland, WA 99354, USA*
[b] *NASA Johnson Space Center Houston, TX, USA*

Available online 17 August 2006

Abstract

A process is presented for in situ resource utilization of indigenous resources on Mars to produce hydrocarbon propellants using microchannel reactors. The proposed system utilizes CO_2 from the atmosphere on Mars and hydrogen brought from Earth. The CO_2 is reacted in a Sabatier reactor (SR) to produce methane (propellant) and water. The water generated is electrolyzed to produce oxygen (oxidant). The hydrogen is recycled. The microchannel SR used in this study consisted of integrated cooling and reaction channels, was <100 cm^3 in volume and 175 g in mass, and used a proprietary catalyst. When operated at 400 °C, 70–80% CO_2 conversion was achieved, which enabled $\sim$0.0125 kg CH_4/h production or one-eighth the target mission-required throughput. The modular design of microchannel reactors would enable simple scale-up to full-scale production for the proposed mission. To produce the desired oxygen-to-methane ratio (3.8 by mass), a reverse water-gas-shift reactor (RWGS) converts CO_2 and hydrogen to water and CO. Again, the water is electrolyzed and the hydrogen recycled; the CO is discarded. The RWGS system contained 30 microchannels in a four-reactor monolith (70 cm^3). When operated at 700 °C and at a contact time of 36 ms, 0.09 kg/h O_2 generation (half-scale production for a sample Direct Robotic Earth Return Mission) was achieved, and 0.18 kg/h (full-scale production) was accomplished when operated at 18 ms.

Keywords: In situ resource utilization; Sabatier reactor; Reverse water-gas-shift reactor; Microchannel reactors

1. Introduction

Over the last decade, analytical studies have indicated that in situ resource utilization (ISRU) may drastically reduce mission payload (mass), cost, and risk for exploration of outer space [1–3]. In addition, ISRU may allow longer missions with increased objectives [1–3]. For example, for a mission to Mars, the initial mass launched from low Earth orbit may be reduced by 20–45% if hydrocarbon propellants are produced using carbon dioxide from the Mars atmosphere and hydrogen brought from Earth [1]. If Mars-supplied water is utilized, even greater reductions are likely.

The hardware used for this in situ propellant production (ISPP) technology must be reliable; robust; compact; and highly thermally, chemically, and electronically efficient [1]. To meet these critical requirements, researchers at the Pacific Northwest National Laboratory (PNNL) and the NASA Johnson Space Center (JSC) are developing chemical and thermal systems based on advances in process intensification and miniaturization. The microchannel-based ISPP system discussed here integrates a CO_2 purifier, concentrator, and compressor, Sabatier reaction (SR), reverse water-gas-shift (RWGS) reaction, and water electrolysis (WE) to produce hydrocarbon propellants using microchannel technology. This paper describes the development of the first-generation RWGS and SR reactors. A novel reactor combining the RWGS and SR reactions is also presented.

2. ISPP process and objectives

Mars has a low-pressure (6–10 Torr), low-temperature (184–242 K) atmosphere, which is mainly carbon dioxide (95.5%) with residual amounts of nitrogen (2.7%), argon (1.6%), and traces of other gas such as oxygen and water (0.15 and <0.03%, respectively) [4]. Potential water sources located at the poles, in the soil, and subterranean reservoirs provide a second major resource [3]. Studies on ISRU [1,5] have shown the importance of large quantities of accessible water. The ISPP process uses water as a source for hydrogen and oxygen, as described in more detail below.

* Corresponding author. Tel.: +1 509 373 1473; fax: +1 509 376 3108.
E-mail address: JD.Holladay@pnl.gov (J.D. Holladay).

0920-5861/$ – see front matter
doi:10.1016/j.cattod.2006.07.019

A conceptual Direct Robotic Earth Return Mars mission [6] was used to develop the amount of fuel and oxygen requirements. The production rate for this mission was approximately 0.38 kg/h of O_2 and 0.1 kg/h of CH_4 for approximately 3000 h of operation. The O_2 and CH_4 mass ratio (3.8:1) was selected in order to achieve efficient propulsion operation. Since mission requirements are constantly being updated, the reactors were designed to show that they can easily be scaled as necessary.

Fig. 1 depicts a schematic of the ISPP system. As shown, the CO_2 is first purified, concentrated, and pressurized to between 0.1 and 5 bar. Next, the CO_2 is mixed with H_2, preheated, and reacted in the SR and the RWGS reactor. Since the SR is exothermic, the reaction is self-sustaining.

$$CO_2 + 3H_2 = CH_4 + 2H_2O \quad \Delta H = -165\,\text{kJ/mol} \tag{1}$$

The H_2O vapor produced is condensed and decomposed in the WE, producing O_2 and H_2. The O_2 is dried and stored, and the hydrogen is recycled. This process produces O_2 and CH_4 at a 2:1 mass ratio; therefore, additional O_2 is needed to reach the 3.8:1 desired ratio. The additional O_2 is produced in the endothermic RWGS reactor.

$$CO_2 + H_2 = CO + H_2O \quad \Delta H = +37.2\,\text{kJ/mol} \tag{2}$$

CO and H_2O are separated in a condenser, and the CO discarded. The H_2O is decomposed in the WE, producing O_2 and H_2.

The schematic is extremely simplified, but illustrates some important aspects of the proposed ISPP system. Increasing efficiency and minimizing thermal and electrical demands requires extensive recuperation and energy cascading from hot unit operations, such as catalytic reactors, to cold operations, such as vapor liquid separation and CO_2 acquisition.

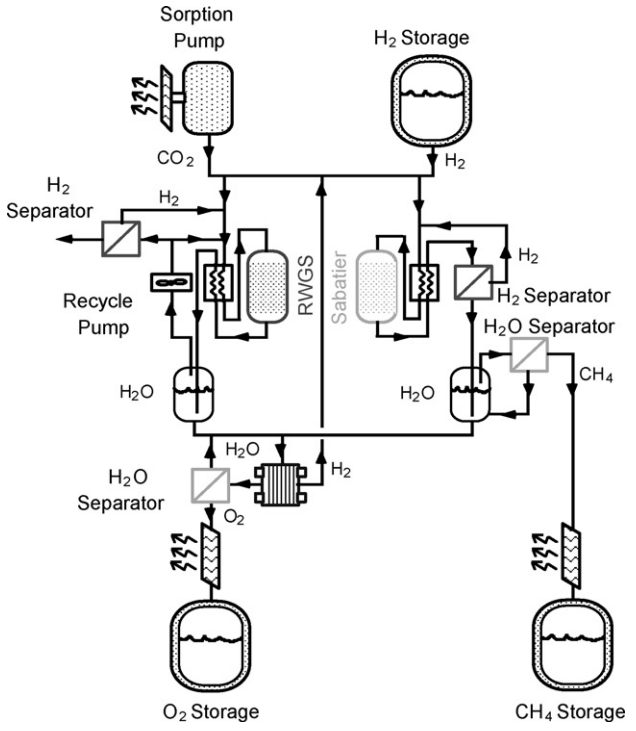

Fig. 1. Mars ISPP system schematic for oxygen/methane production.

For all the subsystems in the ISPP, minimizing the size and weight of the reactors is accomplished by maximizing the activity of catalyst and obtaining high CO_2 conversion. High CO_2 conversion is only possible by controlling the temperature. Since the SR is exothermic, the SR reaction temperature rises under adiabatic conditions as the reaction progresses. Likewise, since the RWGS reaction is endothermic, its temperature falls. In both cases, thermodynamic equilibrium conversion is reduced. Using microchannel architecture, the temperature of these reactions can be controlled to improve conversion and the resultant reactor sizing.

3. Experimental

3.1. Reverse water-gas-shift development

The RWGS was developed in three steps: a single channel catalyst was tested; next, using these results, a multichannel reactor design was developed; then multichannel reactors were tested. The desired catalyst performance reaction was 35–45% conversion of CO_2 with >95% selectivity[1] to CO at a contact times[2] (CT) of ≤0.025 s. For a given conversion, selectivity, and contact time the reactor size could be determined. By using the thermodynamics, the required heat addition was determined and incorporated into the design. Finally, the materials of construction and thickness were determined using the operating temperature and pressure.

The designs for the multichannel reactors were based on sheet architecture [6]. Thin metal shims were machined using photochemical etching and then stacked to form headers, microchannels, and heating passages. The shims were then diffusion bonded to create a single monolith (the lamination fabrication approach used is discussed in more detail in Reference [7]). Conventional machining was used to remove excess material and to expose slots for inserting the catalyst completing the design. Once the catalyst was loaded into the reactor, the reactor was sealed and the feed and product tubing welded between the reactor and heat exchangers.

Testing was performed over a range of temperatures, H_2-to-CO_2 ratios, and contact times. Sub-ambient pressure operation was not possible. Instead, nitrogen was used to dilute the reactive gases to simulate the effect of lower partial pressures of hydrogen and carbon dioxide.

A proprietary supported Ru catalyst made in-house was used. The catalyst was wash-coated onto a FeCrAlY felt using the following method. First, the catalyst powder was ball-milled at 75 rpm for at least 24 h in deionized H_2O using 3-mm ZrO_2 grinding beads with a mass ratio of 1:1 powder to beads in a sealed container. Wire electro discharge machining (EDM) was used to cut the FeCrAlY felts (~0.01 in. thick) to the desired dimensions. Reagent-grade acetone followed by

[1] Unwanted by-products could include coke and methane.

[2] Contact time is the inverse gas hourly space velocity (GHSV) and is based upon the entire reactor volume.

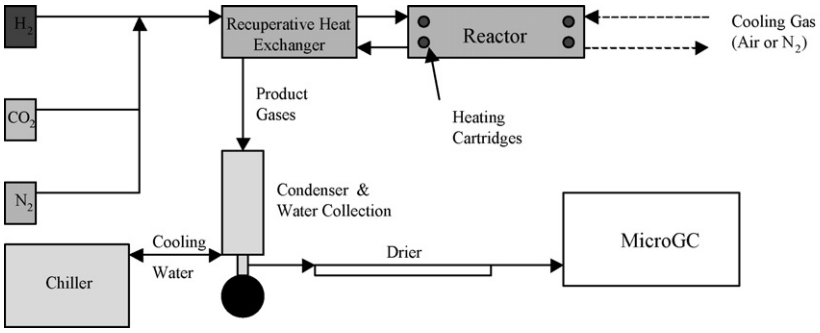

Fig. 2. Multichannel reverse water-gas-shift reactor test stand.

ethanol in an ultrasonic bath was used to clean the felts. After cleaning, the felts were calcined at 500 °C (ramping at 5 °C/min from room temperature) for 2 h to pretreat the surface. The felt thickness was measured at four locations and discarded if the thickness was greater than 0.011 in. or less than 0.009 in. The felts were dipped in the catalyst slurry, air dried, and then weighed. The dipping and air drying were repeated until the target weights were achieved. After the target weights were achieved, the felts were dried at 110 °C in a vacuum (100 mmHg) overnight. Next, the samples were calcined at 500 °C (ramping at 5 °C/min from room temperature) for 2 h.

The single-channel reactor was operated at a temperature of 550–850 °C and atmospheric pressure. The CTs ranged from 18 to 36 ms, with a feed of hydrogen and CO_2 mix between 1:1 and 4:1 molar ratio. After cooling the product gases, water was removed using a condenser followed by Dri-rite. The gases were then analyzed with a dual-column Agilent MicroGC with Poraplot U and mole sieve column using a thermal conductivity detector.

A schematic of the multichannel reactor test stand is shown in Fig. 2. Mass flow controllers (MKS) were used for delivering the hydrogen, CO_2, and nitrogen to a microchannel recuperative heat exchanger. The heat exchanger recovered heat from the product gases to preheat the reactants to near reacting temperature. Cartridge heaters were used to supply the initial heat and maintain the reaction temperature. Product gases then passed back through the recuperative heat exchanger and into a condenser that removed and collected the water generated. A PermaPure gas diffusion dryer was used to further dry the gases, which were then analyzed by the GC.

The RWGS reactor was designed to (1) heat the reactants to the required temperature and supply enough heat to maintain that temperature throughout the endothermic reaction and (2) provide a modular design with easy scale-up, redundancy, and/or turn-down. The RWGS reactor was sized for half the requirements for a Direct Earth Return Mars mission.

The RWGS reactor was built using microchannel architecture and laminate fabrication techniques. The design of one of the reactor shims is shown in Fig. 3. Approximately 30 of each of these shims plus a top and bottom plate were diffusion-bonded together, creating a 2.54-cm-thick monolith. Multiple reactor monoliths could be built to scale-up the process. Each of these reactors could be operated individually to effect turn-down as needed. The cross-hatched areas depicted in Fig. 3 were etched completely through and the shaded areas were etched halfway through the metal. A second shim (the spacer shim) similar to the first was made by completely etching through the metal in the cross-hatched and shaded areas. The spacer shim was placed on top of the flow distributor shim to create the necessary volume for the catalyst. The mirror image of the pictured shim was then placed over the top of the other two shims to create a single open microchannel. This was repeated to form a reactor monolith using 30 shims in this design. A single monolith could be used, or multiple monoliths could be used to scale up the process.

The catalyst was inserted within the reactors inside the large rectangles 2 cm long and 0.5 cm wide. Gas flowed down through the small rectangular preheat channels before entering the catalyst distribution header. These slots allowed the gases to be heated from ~600 °C out of the recuperator to 750 °C before entering the reactor section. The gases then turned and flowed upward in the rectangular catalyst distribution header. The gases exited through the side of the reactor and entered the recuperator. The circular holes in Fig. 3 show where the rod heaters were inserted. Fourteen 1/8 in.-diameter rod heaters were placed along the top and sides of the reactor channels. These rods passed all the way through the reactor and could be heated up to 850 °C. The total volume of the reactor was 67 cm^3, with a mass of approximately 500 g.

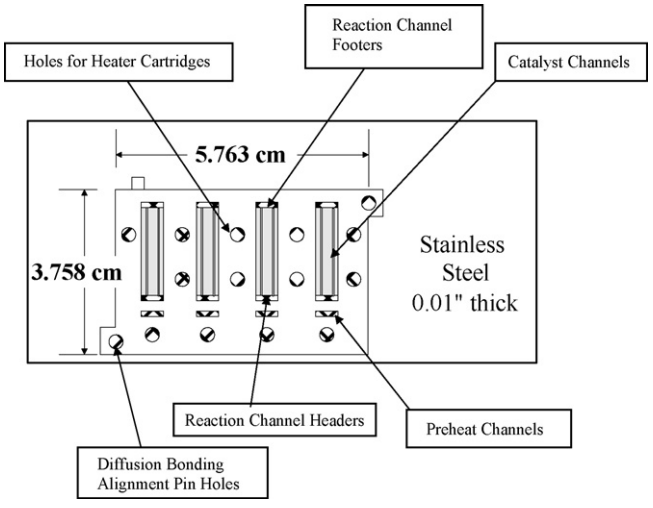

Fig. 3. Flow distributor shim used to fabricate the RWGS reactor.

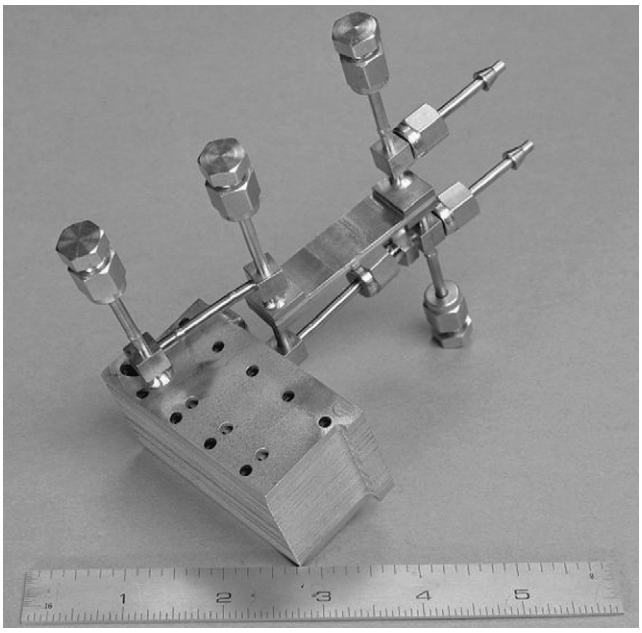

Fig. 4. Completed RWGS reactor. This unit was designed to be half scale for direct Earth return Mars mission requirements.

One recuperative heat exchanger was used for each of four sets of reaction channels. The heat exchangers, 1.37 cm × 5.8 cm × 0.46 cm ($w \times l \times t$), were approximately 90% effective. Each had eight channels (four hot side; four cold side) with a countercurrent flow. Heat was conducted from the heater cartridges through the stainless steel and along the fins between the catalyst channels. Since each of these sets of microchannels was symmetric, only one was tested during these operations. A photograph of the completed unit is shown in Fig. 4.

The reaction temperature was measured with a thermocouple based on the product gas-temperature outlet. The temperature of the gases passing through the heating channel within the reactor block were also measured and found to be within 10 °C of the product gases. No temperature measurements were made in the microchannels themselves. The operating pressure of the reactor ranged from 130 to 180 kPa.

3.2. Sabatier reactor

Similar to the RWGS, the SR was developed in a series of steps: catalyst testing in single-channel reactors, designing multichannel reactors based on the single-channel results, and testing the multichannel reactor. The catalyst performance criterion for testing in the multichannel reactor was >85% conversion of CO_2 with >95% selectivity to CH_4 at a CT of ≤0.1 s. The data provided for the single-channel reactors were then used to assist in the design of the multichannel reactor. Based on the CT, for a given conversion and selectivity, the reactor size could be determined. By using the thermodynamics, the amount of heat rejection or addition could be determined and incorporated into the design. Finally, with the operating temperature and pressure, the materials of construction and thickness could be determined.

Once the reactor was fabricated, testing was performed over a range of temperatures, stoichiometries (H_2/CO_2), and CTs. Again, operating the reactors at sub-ambient pressure was not possible. To simulate the effect of lower partial pressures of hydrogen and CO_2, various N_2:reactive gas mixtures were evaluated.

For the SR, three commercial (Degussa) Ru-based catalysts, designated as catalyst A, B and C2, were evaluated. The catalysts were wash-coated onto a FeCrAlY felt using the following method. The catalyst powder was ball-milled at 75 rpm for at least 24 h in deionized H_2O using 3-mm ZrO_2 grinding beads. The mass ratio of powder to beads was 1:1 in a sealed container. The FeCrAlY felts (∼0.01 in. thick) were prepared by cutting them to the desired dimensions using wire EDM. Next, they were cleaned with reagent-grade acetone followed by ethanol in an ultrasonic bath. The felts were calcined at 500 °C (ramping at 5 °C/min from room temperature) for 2 h to pretreat the surface. The thickness of the felts was measured at four locations and discarded if the thickness was greater than 0.011 in. or less than 0.009 in. The felts were dipped in the catalyst slurry, air dried, and then weighed. The dipping and air drying were repeated until the target weights were achieved. After the target weights were achieved, the felts were dried at 110 °C in a vacuum (100 mmHg) overnight, and then calcined at 500 °C (ramping at 5 °C/min from room temperature) for 2 h.

The single-channel reactor was operated at atmospheric pressure and a temperature of 200–550 °C. The CT ranged from 50 to 200 ms, with a feed of hydrogen and CO_2 mix (4:1 molar ratio). Product gases were cooled and water removed using a condenser followed by Dri-rite. The gases were then analyzed with the dual-column Agilent MicroGC described above.

The layout for the reactor system was essentially the same as for the RWGS reactor shown in Fig. 2. Hydrogen, CO_2, and nitrogen were fed through MKS mass flow controllers to a microchannel recuperative heat exchanger. This ∼90% effective heat exchanger used heat from the product gases to preheat the reactants to near reacting temperature. The gases then reacted with catalysts within the reactor. The heat of reaction was removed by flowing nitrogen or air through interleaved microchannels. Cartridge heaters were used to supply the initial heat and maintain the reaction temperature when operating under low conversion conditions (i.e., heat of reaction not sufficient to maintain temperature). Product gases then passed back through the recuperative heat exchanger and were dried and analyzed as described above.

The single-channel results and equilibrium data were used to develop a design for the SR. Because of the longer contact time as compared to the RWGS, the SR reactor was designed for one-eighth of the scale required for the conceptual mission.

The SR was designed as a combined reactor/heat exchanger. To create the temperature profile needed, conduction down the length of the reactor had to be minimized, which was accomplished by producing a long, thin reactor design with temperature control on each end. The temperature profile was created based on the temperature set at each end. To heat the two ends, four cartridge heaters were inserted into each end.

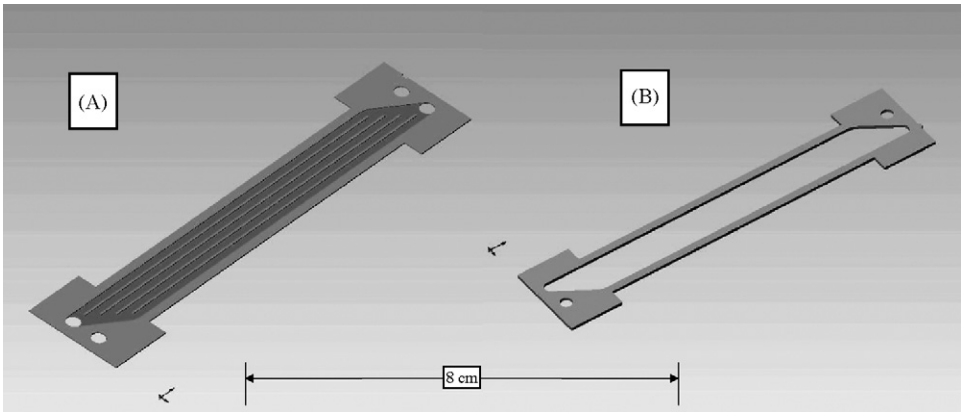

Fig. 5. Sabatier reactor shims. (A) Flow distributor shim and (B) spacer shim.

If cooling was required, cold gas was passed down the microchannels interleaved with the reaction channels. One of three shims used to produce this design is shown in Fig. 5.

To minimize the number of diffusion bonding steps required, three units were etched into a single shim design. After diffusion bonding, the three reactors were cut apart and machined separately. Two main shims were used in the design. The first was etched part way through the metal leaving ribs for support and flow distribution. A second shim (the spacer shim) with the area etched completely through the metal was placed on top of the flow distributor shim to create the necessary volume for the catalyst. The mirror image of the pictured shim was then placed over the top of the other two shims to create a single open microchannel. Separate channels for cooling gas flow were interleaved between the reaction channels. These channels were similar in design, but had different headers. Sets of the reactor and cooling microchannels were diffusion-bonded to a single monolith.

The overall dimensions of this one-eighth-scale reactor are 11 cm × 2.3 cm × 3.7 cm. A photograph of a completed reactor is shown in Fig. 6. Seven reaction microchannels each were used, interleaved with eight cooling microchannels. Each microchannel was created with a top and bottom plate that contained the flow distributors (A) and a spacer shim (B) to provide for the catalyst volume. To initially heat the reactor, electric rod heaters were placed on either end of the reactor. Once the reaction was initiated, these rod heaters could be turned off as the exothermic reaction maintained the reactor temperature. To control the temperature, coolant flow and temperature can be adjusted. The recuperative heat exchanger heats the feed streams with the product streams.

The reaction temperature was measured with K-type thermocouples located at the product gas entrance, the exit, and at four locations axially down the length of the reactor. The experiment was run near atmospheric pressure with a pressure range from 115 to 150 kPa, and operated at 400 °C.

4. Results and discussion

4.1. RWGS single-channel catalyst testing

The results of the single-channel tests are presented in Fig. 7. As can be seen, the CO_2 conversion was below equilibrium for the reaction temperature, but it had a high selectivity to CO. Even with the lower-than-expected conversion, the catalyst did achieve the desired 35–45% conversion at high selectivity (>95% to CO), but at a slightly higher contact time (35 ms compared to the desired of <25 ms). It was believed that some bypass was occurring in the single-channel reactor. This bypass would be eliminated in the multichannel design.

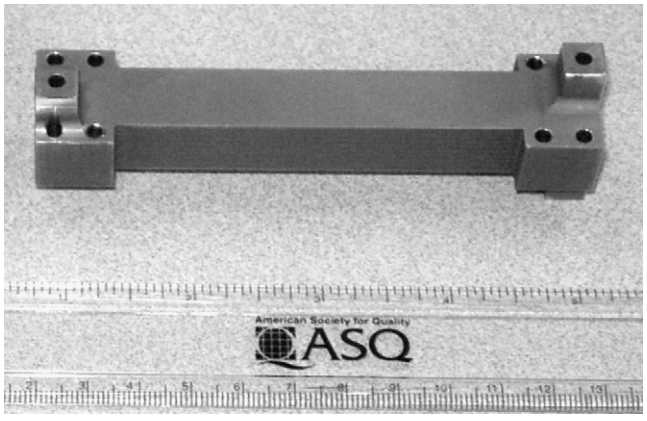

Fig. 6. Completed Sabatier reactor.

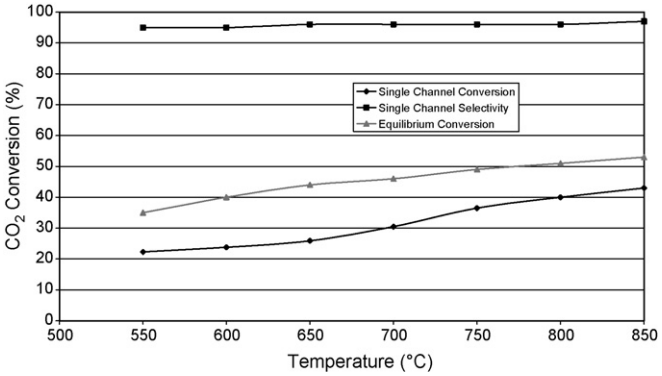

Fig. 7. Single-channel testing of the RWGS engineered catalyst at 35 ms residence time and stoichiometric conditions.

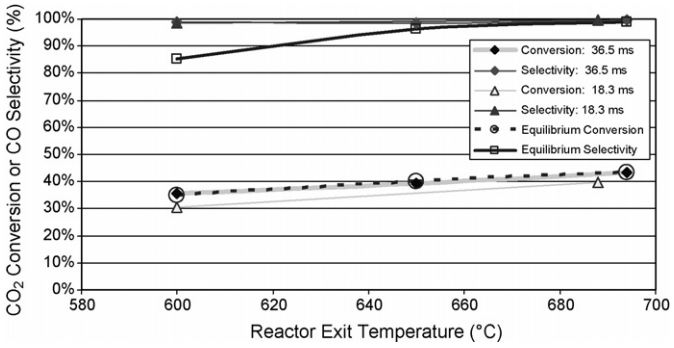

Fig. 8. RWGS reaction CO_2 conversion and CO selectivity at H_2:CO_2 ratio = 1 and contact times of 18.3 and 36.5 ms.

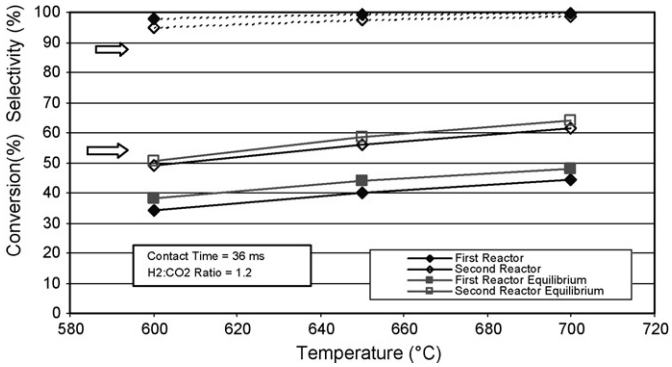

Fig. 10. Conversion and selectivity for two RWGS reactors in series removing the water between to increase conversion. Both reactors are at the same temperature. Experimental results are compared to thermodynamic equilibrium.

4.2. RWGS multichannel reactor

Fig. 8 illustrates CO_2 conversion as a function of temperature and contact time for the multichannel RWGS reactor. Equilibrium conversion and selectivity are also shown. As would be expected, the conversion increases with temperature and decreases with contact time. It should be noted that the conversions for the multichannel reactor are higher than similar conditions with the single-channel reactor. This supports the hypothesis that some of the reactants bypassed the catalyst in the single-channel unit. It also illustrates that the multichannel design can help eliminate bypass, which is found in many conventional reactors. At the design condition of 36 ms CT, the reactor outlet reached equilibrium conditions over the range of temperatures studied here. By doubling the flow rate (to 18 ms CT), the overall reactor is large enough to support throughput for the conceptual sample mission. However, there is a slight decrease in conversion away from equilibrium.

Due to thermodynamic equilibrium, the conversions are constrained to fairly low levels. Fig. 9 illustrates that increasing the concentration of hydrogen increases the conversion of CO_2 beyond that attainable at a 1:1 ratio of H_2 and CO_2. However, at higher H_2:CO_2 ratios, more total gas must be purified and compressed downstream of the reactors to recycle the added hydrogen used during the reaction step. Once the sensitivity of the hydrogen recovery and recycle step with flow rate is better quantified, the H_2:CO_2 ratio can be defined to minimize the overall process size.

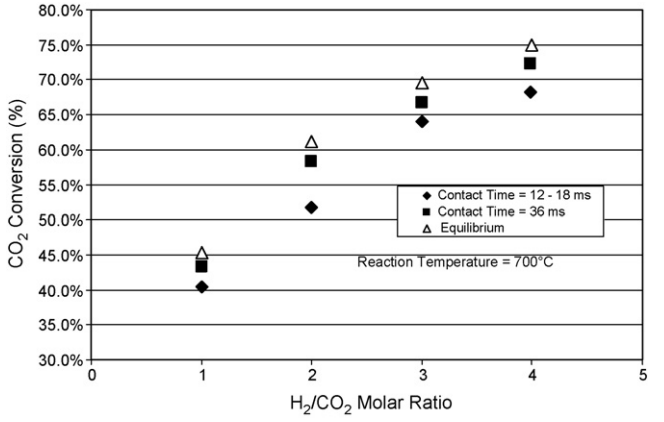

Fig. 9. H_2:CO_2 ratio and contact time effects on CO_2 conversion for the RWGS reaction. Reactor outlet temperature was 700 °C.

If the purification system increases at a faster rate than the reactor system when hydrogen flow rates increase, another approach may be necessary to increase the conversion beyond equilibrium. One approach that was tested successfully is to use two stages of RWGS reactions with a water-separation step between. By removing the water after the first stage of the reaction, the equilibrium conversion of CO_2 can be shifted further towards CO. For the experiment performed, the product from one set of reaction channels was cooled to ~8 °C and the water collected. These gases were then reheated to the original reaction temperature and sent into a second set of reaction channels.

To minimize heat requirements, a recuperative heat exchanger was used for both sets of reactions. The results of this approach as compared to predictions are shown in Fig. 10. The figure shows an increase of approximately 15% in overall conversion by removing the water and reprocessing the reactor products. Furthermore, the conversion obtained is very similar to that predicted by thermodynamic equilibrium.

4.3. Sabatier single-channel test results

Catalyst activities were initially tested in a single-channel reactor loaded with the engineered form of the catalyst. Based on the results (Fig. 11), the highest conversions were possible with the "C2" catalyst. Consequently, this catalyst was selected for further study in the multichannel reactor. Stability and longevity were not addressed in the initial testing.

As can be seen from the equilibrium data in Fig. 11, this reaction reaches high conversions at reduced temperatures. However, the kinetics of the reaction become very slow at these lower temperatures, requiring in increased contact time to reach close to equilibrium conversion. The net result is a requirement of larger reactor.

At higher temperatures, conversion decreases and CO begins to form as a byproduct. To improve conversions, using a microchannel heat exchanger, the Sabatier reactants could be

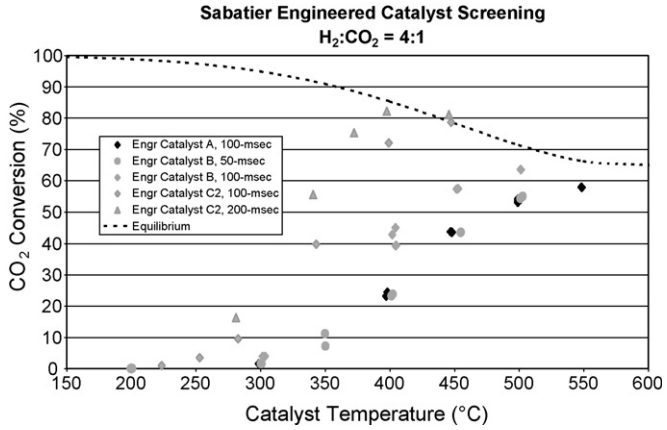

Fig. 11. Results of the engineered Sabatier reaction catalyst in a single-channel reactor.

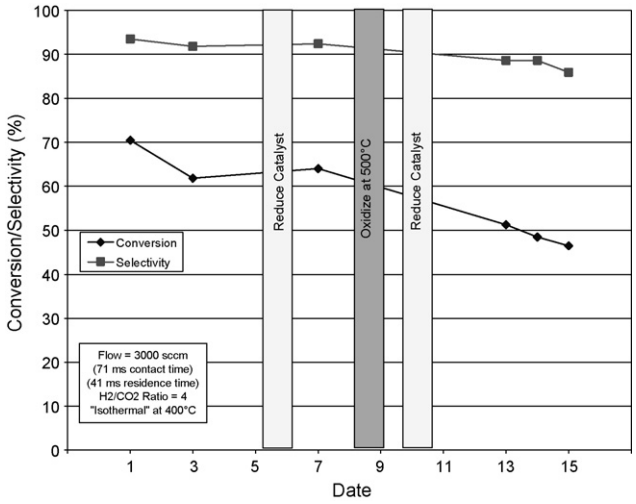

Fig. 13. Deactivation of the SR catalyst over time.

preheated to between 550 and 600 °C before the reactor. At these temperatures, fast kinetics will result in the majority of the conversion occurring in a short residence time. As the gases react, they could then be cooled using the countercurrent flow of coolant, where the final product will exit with nearly complete conversion found at these lower temperatures. Because the Sabatier reaction is exothermic, both heat of reaction and sensible heat must be removed down the length of the reactor.

4.4. Sabatier reactor multichannel reactor testing

The multichannel SR was evaluated over a range of temperatures and CTs at a constant H_2:CO_2 ratio of 4 (stoichiometric). Due to the exothermicity of this reaction, in some cases, it was difficult to maintain the reactor isothermal. In general, the first axial temperature was 20–30 °C higher than the subsequent temperatures down the length of the reactor. This problem was exacerbated at lower CTs.

The initial experimental results are shown in Fig. 12. For comparison, the isothermal equilibrium case and the adiabatic equilibrium case are also plotted. At a contact time of ∼400 ms, the CO conversion is within experimental error of the equilibrium conversion of 84.9%. As expected, the conversion

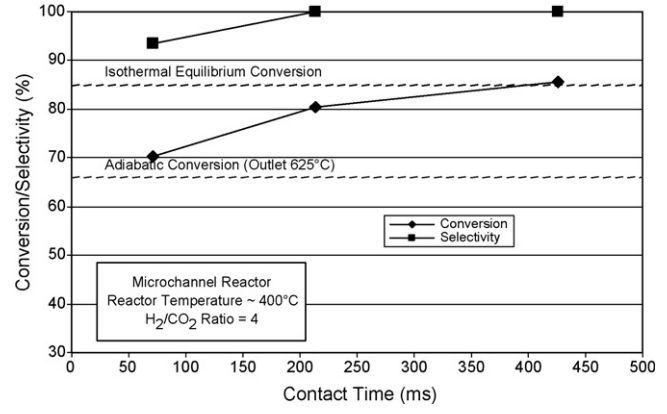

Fig. 12. Conversion and selectivity of the SR compared to thermodynamic calculations.

decreases at lower contact times. To achieve the methane production for one-eighth scale of the sample return mission with this reactor, a CT of approximately 100 ms is required. This would result in slightly more than 70% conversion in the reactor. These values are less than the target performance criterion. By controlling the temperature of the reactor to close to isothermal rather than allowing it to operate adiabatically and by increasing the contact time, the CO_2 conversion increased from a possible 66% to over 80%, thus achieving the desired conversion targets.

Over the course of several days of experimentation, there was a steady decline in the catalyst activity (Fig. 13), and several approaches were taken to improve it. If the reduction in activity were associated with the catalyst becoming oxidized, reduction would have improved the conversion. If it were coking, the oxidation and re-reduction of the catalyst would have improved the performance. Based on the results that these approaches did not recover catalyst activity, catalyst sintering may be the reason for the decline.

4.5. Novel integrated SR and RWGS reactor

Since the SR is exothermic and the RWGS reaction is endothermic, the energy from one system could be transferred to the other. Interleaving the catalyst materials and operating in a countercurrent flow mode would cool the SR catalyst as it moved down the reactor by adding heat to the endothermic RWGS reaction. The RWGS reaction gases, in turn, would be heated as they moved down the channel by the exothermic SR. In both cases, it may be possible to improve reaction conversion. Additionally, this approach would minimize the cooling required for the SR and the heating required for the RWGS, reducing the total energy consumption. The ability to operate with SR only, RWGS only, or both reaction run simultaneously was incorporated into the design.

To test this hypothesis, seven channels of the SR reactor were filled with SR catalyst and the interleaved eight channels were filled with the RWGS catalyst. Gases were plumbed to flow countercurrent and both gases were preheated with

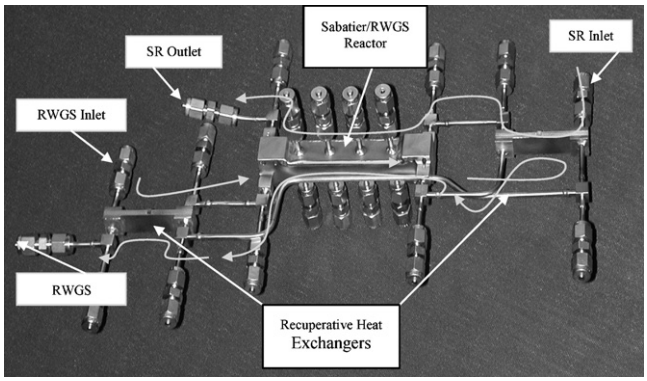

Fig. 14. The combined RWGS/SR with associated recuperative heat exchangers. Both the reactor and the heat exchangers operate in the U-configuration (gases exit on the same side as they enter).

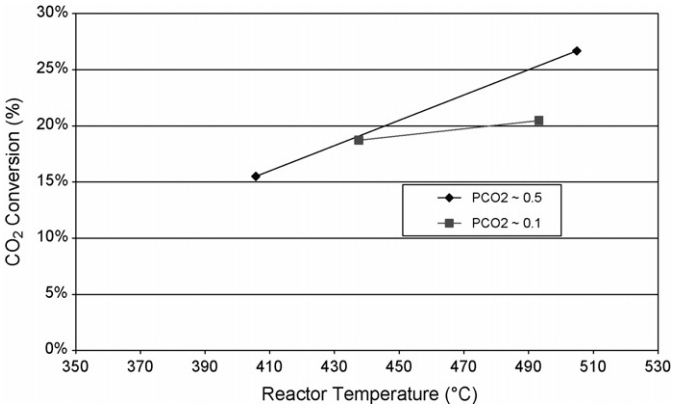

Fig. 16. Comparison of CO_2 conversion as a function of partial pressure and temperature for the same CO_2 and H_2 throughput rate.

recuperative heat exchangers. The reactor/recuperative heat exchanger configuration is shown in Fig. 14. Because the SR flow rates are lower than the RWGS to meet the NASA ratio requirements, there is more sensible heat associated with the RWGS than the SR. The RWGS products were then used to preheat both the RWGS and SR feed.

4.5.1. Integrated reactor–RWGS operation

Before the combined reactors were run, each reaction was performed to better understand the conditions of operation in this configuration. Previous testing with the RWGS was conducted primarily at temperatures greater than 600 °C. In order to study the SR, especially if deactivation due to sintering would be a problem, the RWGS reaction would need to be operated at less than 550 °C. Furthermore, the highest SR conversions occur at ~400 °C. Thus, initial testing of the eight-channel RWGS reactor was performed at these conditions with nitrogen flowing in the SR channels. This second set of tests also studied the effect of partial pressure of reactants on conversion. Due to the equipment size and energy costs for compression of the CO_2, lower pressures should be considered. Because of equipment constraints, the system was not operated at less than atmospheric pressure. Instead, nitrogen was added to the system as a diluent. Results were then compared to a process with the same throughput rate.

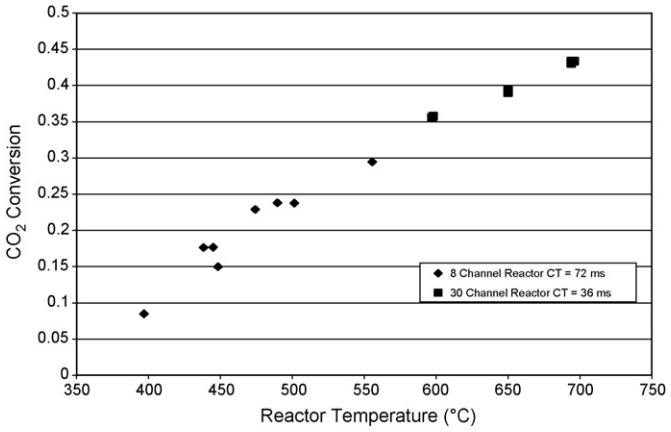

Fig. 15. Comparison of conversion results of eight-channel RWGS reactor and previous tests of 30-channel RWGS reactor.

A comparison of the 30-channel data discussed above and the eight-channel RWGS data is presented in Fig. 15. The results are comparable for the two systems, although no overlapping data were taken. At the lower temperatures, the kinetics are sufficiently slow that longer CTs are required.

The partial pressure experimental results for the RWGS are shown in Fig. 16. Reaction kinetic models generally indicate the reaction rate is proportional to the partial pressure of the reactants [6]. Therefore, the reaction rate and thus the conversion would be expected to be lower at lower partial pressures for a constant reactant flow rate. However, the results indicate little reduction in conversion with a fivefold decrease in reactant partial pressure. Such a result would allow a decrease in pressure to the RWGS reactor without a significant effect to the conversion. In addition, the lower partial pressure resulted in higher selectivity to CO, which would reduce the load on the separations equipment downstream of the reactors.

4.5.2. Integrated reactor–SR performance

Using the combined reactor and nitrogen flowing through the RWGS channels, the SR was also studied. Similar to the RWGS reaction, the conversion was studied for lower partial pressures. The results of this comparison are shown in Table 1. As can be seen, both the conversion and the selectivity decrease at the lower reactant gas partial pressure. Thus, for this particular reaction, there would be less benefit in reducing the pressure of the inlet gases than for the RWGS reaction.

4.5.3. Integrated SR and RWGS operation

The integrated reactor was tested over a wide range of conditions. Operating both reactors simultaneously created a

Table 1
Effect of reactant partial pressure on the Sabatier reaction*

P_{CO_2} (atm)	CO_2 conversion (%)	CH_4 selectivity (%)
0.23	69	91
0.063	41	71

* Tests performed at H_2:CO_2 = 4:1, ~450 °C, and CO_2 flow of 123 sccm.

Table 2
Combined SR/RWGS Reactor Results Summary

Experimental conditions	Run 1	Run 2	Run 3	Run 4	Run 5	Run 6
T_1 (°C)	381	378	378	378	556	532
T_2 (°C)	515	564	553	551	556	532
RWGS H_2:CO_2	1	1	2	1	1	–
RWGS contact time (ms)	72	72	96	144	72	–
RWGS conversion (%)	18	23	35	26	29	–
RWGS CO selectivity (%)	84	87	74	84	90	–
RWGS production rate[a] (%)	47	62	40	34	82	–
SR H_2:CO_2	6	4	6	6	–	6
SR contact time (ms)	200	100	100	198	–	100
SR conversion (%)	76	52	63	78	–	74
SR CH_4 selectivity (%)	95	85	89	94	–	81
SR production rate[a] (%)	37	62	57	37	–	63

[a] Percentage of required production rate to meet sample return requirements of 1/8 scale.

temperature profile along the reactor length to provide high temperatures for the inlet to the SR and the outlet to the RWGS. By adjusting the flow rate of both the reactions, the heat of reaction could more or less be balanced, and the fraction of CH_4 and H_2O could be balanced at the proper ratio. The results of this testing is shown in Table 2. Runs 1–4 are run in a differential temperature mode of roughly the same magnitude, while Runs 5 and 6 are individual reactions run isothermally for comparison. The data in Table 1 illustrate that with an increase in H_2:CO_2 ratio and contact time, both the RWGS and SR reaction conversions increase. The selectivity of these reactions towards CH_4 increases with an increase of these same parameters. In contrast, the fraction of the required one-eighth scale of the Direct Robotic Earth Return Mission (''Production Rate'') decreases with increased H_2:CO_2 ratio and CT. Thus, there must be an optimization between obtaining high production and obtaining high conversion.

The isothermal case and differential case can be compared for the RWGS and SR by comparing Runs 2 and 5 and Runs 3 and 6, respectively. The differential case results in a decrease in both conversion and production rate as compared to the isothermal case. This result is not surprising for the endothermic RWGS reactor, where higher temperatures will result in higher conversion and selectivity. For the SR case, the result is less expected. It indicates that equilibrium conversion is not being reached at the high temperature front end of the reactor, which allows the equilibrium conversion to increase as the temperature decreases further down the reactor. Instead, the reaction is being quenched prematurely, resulting in reduced conversion. This is probably due to the catalyst deactivation that occurred.

By using the differential temperature reactor, the SR and RWGS reactions can be coupled thermally and minimize the amount of heat required to the RWGS by using the heat generated by the SR. A plot of the heat generated by the SR as compared to the heat required for the RWGS is shown in Fig. 17 as a function of specific methane productivity. As can be seen from the figure, for a range of reactor throughputs and the required water:methane product ratio of 3.8, the amount of heat required within the reactor by the RWGS is less than the amount

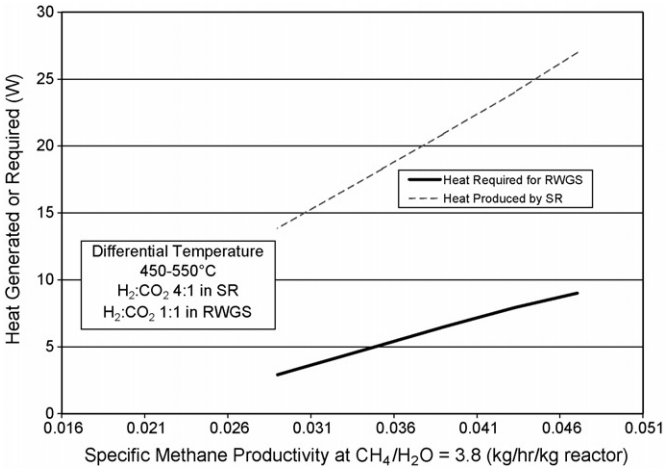

Fig. 17. Comparison of heat generated by the SR and heat required by the RWGS as a function of specific methane productivity at the required methane:-water ratio.

produced by the SR system. This would indicate that with minimal heat losses the reactions could be operated with little or no heat input, which would significantly reduce the energy requirements on the overall system.

The reaction system could be optimized alone to improve conversion and selectivity in terms of temperature, throughput rate, and H_2:CO_2 ratio. However, to minimize overall mass of the entire production plant, these parameters should be optimized to account for the size of the CO_2 collection and product separations systems as well. In the case of the SR and RWGS reactions, by increasing the throughput rate per unit volume of reactor, the required size of the reactor decreases. However, the conversions for the two reactions decrease as well. This results in a lower concentration of product gases (CH_4, CO, and H_2O) in the final product, making them more difficult to extract from the large amounts of reactant gases (H_2 and CO_2). Fig. 18 compares the mass of the reactor based on a scaled mass of the prototype to the fraction of product gases.

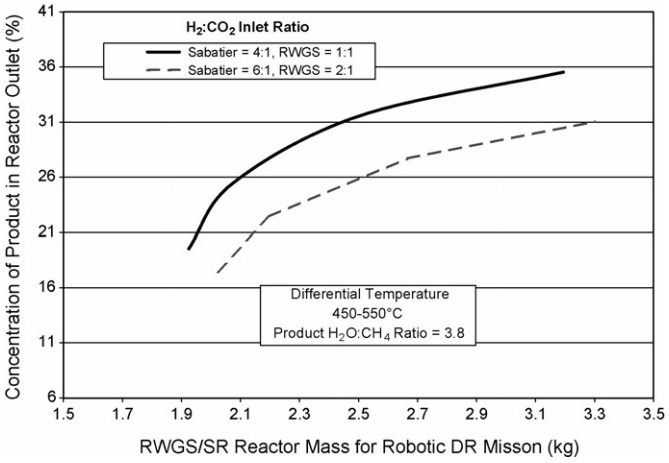

Fig. 18. Concentration of product in the reactor outlet as a function of reactor mass. By increasing the reactor throughput rate, the mass of the SR and RWGS reactors can be decreased. This then causes a decrease in the concentration of the product gases in the reactor output.

Based on these results, if high gas throughputs are attempted to make the reactor mass decrease, the concentration of product gases quickly decreases. In contrast, as the gas throughput decreases sufficiently, eventually equilibrium is reached in the reactors and additional reactor size does not further increase the concentration of products in the reactor effluent.

A similar issue exists with the H_2:CO_2 ratio. At higher H_2:CO_2 ratios, both the SR and the RWGS reactions increase in conversion; however, more total H_2 passes through the reactors unreacted. Thus, the total product gas concentration also decreases, resulting again in a larger separation system.

5. Conclusions

A RWGS Ru/CeO-ZrO_2 catalyst, prepared in-house, was found to be robust over a wide range of conditions and showed no deactivation during testing in a microchannel reactor. Based on the single-channel testing results, a 30-channel reactor RWGS monolith was designed and built. By operating the RWGS reaction at 700 °C, conversions of greater than the targeted 45% were achieved at 36 ms CT. At these temperatures and throughput rates, the 30-channel/4-reactor RWGS monolith would be capable of half-scale throughput for the mission considered here in a total reactor volume of less than 70 cm^3. When the reactor was operated at 18 ms CT, the reactor was capable of full-scale production. Due to equilibrium constraints, higher conversions could not be obtained in a single reactor. However, by adding a second reactor in series with water removal between the two reactors, the maximum conversion was increased to 60%. Based on these results a second-generation reactor is under development, which will be smaller, lighter, and more efficient.

A microchannel SR was also developed for an ISPP system. The seven-channel SR reactor was designed to one-eighth scale throughput rate for the sample mission. By operating the reactor at 400 °C, conversions between 70 and 80% could be achieved. Three Degussa Ru-based commercial catalysts were evaluated (A, B, and C2), with C2 being selected for its high activity. However, the catalyst deactivated over time. Results suggest that catalyst sintering and losing surface area may be the cause of deactivation.

A novel reactor that integrated the SR with the RWGS was also tested, and shows promise for reducing the total energy required for operating the system. Additional system studies and further tests will be required to evaluate this approach.

Acknowledgment

This work has been funded by NASA and their support is gratefully acknowledged.

References

[1] G.B. Sanders, T.A. Peters, R.S. Wegeng, W.E. TeGrotenuis, S.D. Rassat, K.P. Brooks, S. Stenkamp, AIAA Report AIAA 2001-0939, 2000.
[2] A.G. Accettura, C. Bruno, S. Casotto, F. Marzari, Acta Areonautica 54 (2004) 471.
[3] G. Chamitoff, G. James, D. Baker, A. Dershowitz, Acta Astronautica 56 (2005) 756.
[4] S.J. Hoffman, D.L. Kaplan (Eds.), Human Exploration of Mars: The Reference Mission of the NASA Mars Exploration Study Team, NASA, July 1997 (SP-6107).
[5] K. Pauly, G.B. Sanders, J.R. Trevathan, D.I. Kaplan, T.A. Peters, R.S. Baird, J.S. Cook, M.L. McClean, Development of in-situ consumable production (ISCP) for Mars Robotic and Human Exploration at the NASA/Johnson Space Center, in: 00ICES-168, 30th Int. Conf. on Env. Systems, Toulouse, France, 2000.
[6] K.P. Brooks, S.D. Rassat, W.E. TeGrothenhuis, Development of a Microchannel In Situ Propellant Production System. PNNL-15456, Pacific Northwest National Laboratory, Richland, WA, 2005.
[7] D.W. Matson, P.M. Martin, D.C. Stewart, A.Y. Tonkovich, M. White, J.L. Zilka, G.L. Roberts, Fabrication of microchannel chemical reactors using a metal lamination process, in: W. Ehrfeld (Ed.), Microreaction Technology: Industrial Prospects. IMRET 3: Proceedings of the Third International Converence on Microreaction Technology, Frankfurt, Germany, 2000.